Int J Legal Med (2014) 128:779–786
DOI 10.1007/s00414-014-1001-5

ORIGINAL ARTICLE

The time-dependent expression of α7nAChR during skeletal muscle wound healing in rats

Yan-Yan Fan · Shu-Tao Zhang · Lin-Sheng Yu · Guang-Hua Ye Ke-Zhi Lin · Shu-Zhen Wu · Miao-Wu Dong · Jun-Ge Han Xiang-Ping Feng · Xing-Biao Li

Received: 16 December 2013 / Accepted: 16 April 2014 / Published online: 30 April 2014

Abstract The study on time-dependent expression of α7 nicotine acetylcholine receptor (α7nAChR) was performed by immunohistochemistry, Western blotting, and real-time PCR during skeletal muscle wound healing in rats. Furthermore, co-localization of α7nAChR with macrophage or myofibroblast marker was detected by double immunofluorescence. A total of 50 Sprague–Dawley male rats were divided into control and contusion groups (3 h, 6 h, 12 h, 1 day, 3 days, 5 days, 7 days, 10 days, and 14 days post-injury). In the uninjured controls, α7nAChR positive staining was observed in the sarcolemma and sarcoplasm of normal myofibers. In wounded specimens, a small number of polymorphonuclear cells, a number of macrophages and myofibroblasts showed positive reaction for α7nAChR in contused zones. Morphometrically, the average ratios of α7nAChR-positive cells were over 50 % from 3 to 10 days after contusion, and exceeded 60 % at 5 and 7 days post-injury. Besides, the positive ratios of α7nAChR were <50 % at the other posttraumatic intervals. By Western blotting analysis, the average ratio of α7nAChR protein expression maximized at 7 days after injury, which was >2.13. Similarly, the relative quantity of α7nAChR mRNA expression peaked at 7 days post-wounding as compared with control by real-time PCR detection, showing a relative quantity of >2.65. In conclusion, the expression of α7nAChR is upregulated and temporally distributed in macrophages and myofibroblasts during skeletal muscle wound healing, which might be closely involved in inflammatory response and fibrotic repair after injury. Moreover, α7nAChR is promising as a useful marker for wound age determination of skeletal muscle.

Keywords Wound age determination · Skeletal muscle contusion · α7nAChR · Forensic pathology

Y.-Y. Fan (✉) · L.-S. Yu · G.-H. Ye · K.-Z. Lin · S.-Z. Wu · M.-W. Dong · J.-G. Han · X.-P. Feng · X.-B. Li
Department of Forensic Medicine, School of Basic Medical Science, Wenzhou Medical University, Wenzhou, Zhejiang Province 325035, People's Republic of China
e-mail: yyfan998@163.com

Y.-Y. Fan · L.-S. Yu · G.-H. Ye · K.-Z. Lin · S.-Z. Wu · M.-W. Dong · J.-G. Han · X.-P. Feng · X.-B. Li
Institute of Forensic Science, Wenzhou Medical University, Wenzhou, Zhejiang Province 325035, People's Republic of China

S.-T. Zhang
Institute of Forensic Science, Heilongjiang Public Security Department, Harbin, Heilongjiang Province 150008, People's Republic of China

Introduction

In forensic practices, wound age determination is one of the most important tasks for forensic pathologists [1–3]. It is well established that a variety of biological substances are involved in wound healing. Some of these substances can be useful markers for the examination of skin wound age [1, 4–7]. However, it is also necessary to give an opinion on the age of skeletal muscle injuries in some cases [8, 9]. Generally, skeletal muscle wound healing is composed of degeneration, inflammation, regeneration, and fibrosis phases [10]. The healing process, which is initiated on injury, requires an elaborate interplay among distinct cell types to orchestrate a series of biological events. These events contain necrosis of the damaged muscle, recruitment of inflammatory cells, as well as appearance of myofibroblasts to form fibrotic lesion [10, 11].

The cholinergic system consists of acetylcholine (ACh), muscarinic and nicotinic receptors (mAChRs and nAChRs), choline acetyl-transferase (ChAT), and acetyl-cholinesterase (AChE) [12]. The α7 nicotine acetylcholine receptor (α7nAChR) is a major subtype of nAChRs. It is generally acknowledged that α7nAChR is expressed by neurons where it plays an important role in modulating neurotransmission [13]. However, increasing

evidences have demonstrated that α7nAChR is also distributed in numerous nonneuronal cell types [12, 14–16], indicating that it may contribute to diverse physiopathological processes. Recently, a close involvement of α7nAChR has been showed in the inflammatory reaction and tissue repair. For example, α7nAChR expressed by macrophages exhibits an essential role in the cholinergic anti-inflammatory pathway [17]. Activation of α7nAChR reduces acid-induced acute lung injury [18]. Besides, α7nAChR can participate in regulation of myofibroblast differentiation and collagen expression during skin wound healing [19]. These observations imply that α7nAChR may be involved in skeletal muscle wound-healing process.

In the present study, we investigated the dynamic expression and distribution of α7nAChR after trauma to skeletal muscle, with special emphasis on the immunolocalization of α7nAChR in macrophages and myofibroblasts. Moreover, time-dependent expression of α7nAChR was examined by immunohistochemistry, Western blotting, and real-time PCR for its practical applicability as a marker to wound age determination of skeletal muscle.

Materials and methods

Animal model of skeletal muscle contusion

A total of 50 healthy, adult Sprague–Dawley (SD) male rats, weighing 280–320 g, were used. Establishment of the standardized animal model of skeletal muscle contusion in rats has been described previously, which was controllable and reproducible well using a self-designed mechanical weight-drop device [9, 20, 21]. Briefly, 45 rats were anesthetized and placed on experimental table in a prone position. Subsequently, a 500-g counterpoise was raised and fell onto the right posterior limb of rats at energy of 2.25 J. After injury, each rat was housed individually, then were killed by a lethal dose of pentobarbital (350 mg/kg) at 3 h, 6 h, 12 h, 1 day, 3 days, 5 days, 7 days, 10 days, and 14 days after injury (5 rats at each posttraumatic interval). Muscle sample was dissected from wound site and equally divided into two parts in each rat. One part was used for immunohistochemical procedure, and another was used for Western blotting and real-time PCR, respectively. For the five control rats, specimens were harvested from the same site after anesthetization with overdose of pentobarbital.

Experiments were conformed to the "principles of laboratory animal care" (National Institutes of Health published no 85-23, revised 1985) and were performed according to the guidelines for the care and use of laboratory animals of Wenzhou Medical University.

Antibodies

The following monoclonal antibodies (mAbs) and polyclonal antibodies (pAbs) were commercially obtained: rabbit anti-α7nAChR pAb (ab10096, Abcam, Cambridge, UK), mouse anti-Macrophage Marker (MAC387) mAb (sc-66204, Santa Cruz Biotechnology, CA, USA), mouse anti-α-SMA mAb (MS-113, Lab Vision Corporation, Fremont, CA, USA), horseradish peroxidase-conjugated goat anti-rabbit IgG (sc-2004, Santa Cruz Biotechnology, CA, USA), biotinylated donkey anti-rabbit IgG (ab6801, Abcam, Cambridge, UK), and Alexa Fluor® 488-labeled donkey anti-mouse IgG (A21202, Invitrogen, CA, USA). Beside, streptavidin, Alexa Fluor® 555 conjugate (S-21381) and Hoechst33258 (H3569) were purchased from Invitrogen.

Immunohistochemical staining and morphometric analysis

The skeletal muscle specimens were fixed in 4 % paraformaldehyde solution with phosphate-buffered saline (PBS; pH 7.4) and embedded in paraffin, followed by sectioning at a thickness of 5 μm. After deparaffinization, the endogenous peroxidase was blocked and antigen retrieval was performed. Nonspecific binding was also removed by incubation with normal goat serum. Afterwards, the samples were incubated with rabbit anti-α7nAChR pAb (dilution 1:500), followed by incubation with Histostain-Plus Kit according to the manufacturer's instructions. As the controls for immunostaining procedures, some sections were incubated with normal rabbit IgG or PBS in place of the primary antibody. No false positive reaction was detected in the sections.

For the analysis of α7nAChR-positive ratio, infiltrating cells of wound zones were evaluated, including polymorphonuclear cells (PMNs), mononuclear cells (MNCs) and fibroblastic cells (FBCs). In each wounded specimen, the average ratio of the number of α7nAChR-positive infiltrating cells to the total number of infiltrating cells was evaluated and expressed as percentage. Two forensic pathologists independent of the experiments were responsible for cell counting and data analysis.

Double indirect immunofluorescent procedures for co-localization

To identify the expression of α7nAChR in macrophages and myofibroblasts, the following double immunofluorescent procedures were conducted. Briefly, deparaffinized sections were blocked with 5 % BSA and incubated with rabbit anti-α7nAChR pAb (dilution 1:200). Thereafter, the sections were incubated with biotinylated donkey anti-rabbit IgG (dilution 1:200) and streptavidin, Alexa Fluor® 555 conjugate (dilution 1:400). Then, tissue sections were further incubated with mouse anti-Macrophage Marker (MAC387) mAb (dilution 1:50) or mouse anti-Myofibroblast Marker (α-SMA) mAb (dilution 1:100). After incubation with Alexa Fluor® 488-labeled donkey anti-mouse IgG (dilution 1:200) at room temperature for 2 h, the nuclei were counterstained with Hoechst 33258. Normal rabbit or mouse IgG was used instead

of primary antibodies as negative control. The sections were mounted and observed under a fluorescence microscope. The immunofluorescent images were digitally merged.

For positive cell ratio evaluation, the average ratio of α7nAChR-positive cells to the total number of cells in each positive cell type was calculated and expressed as percentage.

Protein preparation and immunoblotting assay

The skeletal muscle specimens were homogenized with a sonicator in RIPA buffer containing protease inhibitors at 4 °C. Homogenates were centrifuged, and the resulting supernatants were collected. After protein concentration was determined, aliquots of the supernatants were diluted in an equal volume of 5× electrophoresis sample buffer and boiled for 5 min. Protein lysates (40 μg) were separated on a SDS-polyacrylamide electrophoresis gel and transferred onto PVDF membranes. After being blocked with 5 % nonfat dry milk in TBST at room temperature, the membranes were incubated with rabbit anti-α7nAChR pAb (dilution 1:1,000) and horseradish peroxidase-conjugated goat anti-rabbit IgG. The blots were visualized with Western blotting luminol reagent by electrophoresis gel imaging analysis system. Subsequently, densitometric analyses of the bands were semiquantitatively conducted using Scion Image Software. The relative protein levels were calculated by comparison with the amount of glyceraldehyde 3-phosphate dehydrogenase (GAPDH) as a loading control.

Total RNA extraction and real-time fluorescent quantitative PCR

Total RNA was extracted from the skeletal muscle specimens with RNAiso Plus according to the manufacturer's instructions. The RNA pellet was air-dried for 5 min and resuspended in 30 μl of diethylpyrocarbonate-treated dH_2O. OD values for each RNA sample were measured by ultraviolet spectrophotometer. A260/A280 ranged from 1.8 to 2.0. The RNA was reversely transcribed into cDNA using PrimeScriptTM RT reagent Kit. cDNA synthesis was performed in a 20-μl reaction mixture. The resulting cDNA was used for real-time PCR with the sequence-specific primer pairs for α7nAChR and GAPDH (Table 1). Real-time PCR amplification was performed by Applied Biosystems 7500 Real-Time PCR System using SYBR® PrimeScript™ RT-PCR Kit. To exclude any potential contamination, negative controls were also performed with dH_2O instead of cDNA during each run. No amplification product was detected. The real-time PCR procedure was repeated at least three times for each sample.

Statistical analysis

Data were expressed as means±standard deviation (SD) and analyzed using SPSS for Windows 13.0. The one-way ANOVA was used for data analysis between two groups. Difference associated with $P<0.05$ was considered statistically significant.

Results

Immunohistochemical examination and morphometric analysis

In the control skeletal muscle specimens, infiltrating cells were absent, and a weak α7nAChR-positive staining was detected in the sarcoplasm and sarcolemma of rat skeletal muscle (Fig. 1a). In the wounded samples, a small number of PMNs and MNCs showed α7nAChR immunoreactivity from 3 to 12 h post-injury. At 1 and 3 days, a number of MNCs were positively immunostained with anti-α7nAChR antibody (Fig. 1b). From 5 to 14 days post-wounding, α7nAChR immunoreactivity was mainly detected in regenerated multinucleated myotubes (Fig. 1c) and FBCs (Fig. 1d).

Morphometrically, the average ratios of α7nAChR-positive infiltrating cells increased prominently in the wound zones from 12 h post-wounding, peaked at 7 days after injury, and then was gradually reduced from 10 to 14 days post-wounding. The α7nAChR-positive ratios were over 50 % from 3 to 10 days post-wounding and exceeded 60 % at 5 and 7 days post-injury. Besides, the positive ratios of α7nAChR were <50 % at the other posttraumatic intervals (Table 2).

Cellular localization of the α7nAChR using immunofluorescent staining

By double immunofluorescent staining, the majority of α7nAChR-positive MNCs was found to express macrophage marker (MAC387). At 1 and 3 days after injury, a number of α7nAChR-positive macrophages accumulated in the wound sites (Fig. 2). With extension of wound age, the less

Table 1 Primer sequences used for real-time fluorescent quantitative PCR

Gene	GenBank accession	Primer	Nucleotide sequence	Position	Product size (bp)
α7nAChR	No. L31619.1	Forward:	5′-AGC TGA GTG CAG GTG CTG G-3′	1131-1149	68
		Reverse:	5′-CAG GCC TCG GAA GCC AA-3′	1198-1182	
GAPDH	No. NM_017008.4	Forward:	5′-GGC ACA GTC AAG GCT GAG AAT G-3′	241-262	143
		Reverse:	5′-ATG GTG GTG AAG ACG CCA GTA-3′	383-363	

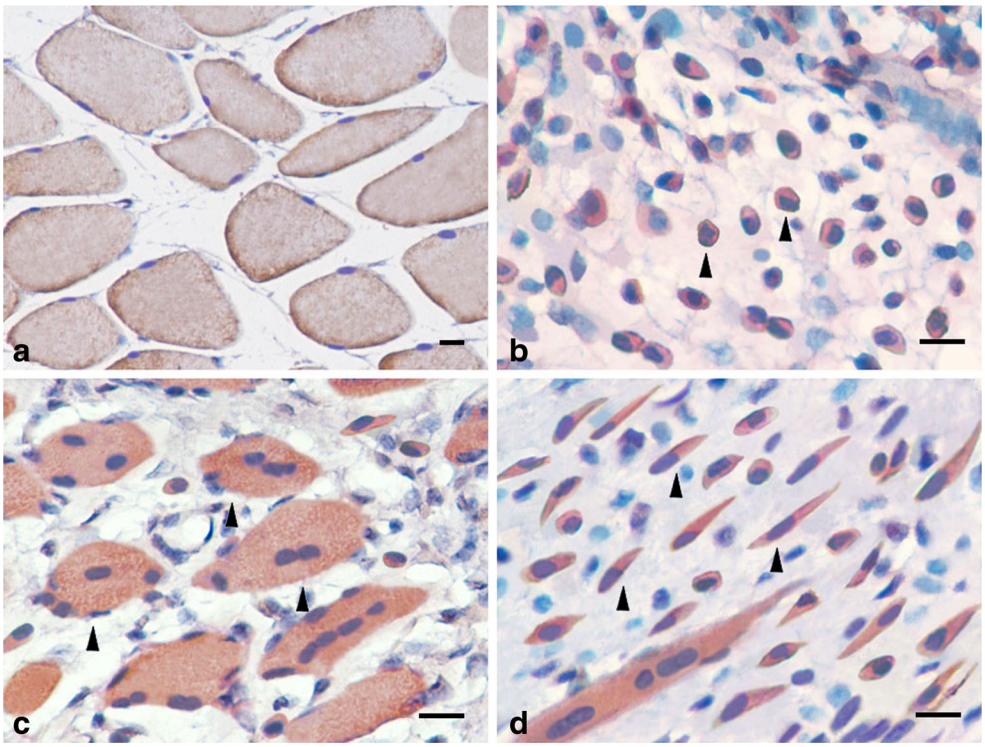

Fig. 1 Immunohistochemical staining of α7nAChR in rat skeletal muscle samples. **a** The weak expression of α7nAChR is detected in the sarcolemma and sarcoplasm of normal myofibers in the uninjured control. **b** The infiltrating MNCs (*arrowheads*) reveal α7nAChR-positive staining at 3 days post-injury. **c** α7nAChR immunoreactivity is found in regenerated multinucleated myotubes (*arrowheads*) at 5 days post-injury. **d** FBCs (*arrowheads*) are positively immunostained with antibody against α7nAChR in the wounded area at 7 days post-injury (*Scale bar*=10 μm)

α7nAChR-positive macrophages were detectable at the wound zones. For the identification of α7nAChR-positive FBCs, co-localization of α7nAChR and myofibroblast marker (α-SMA) was also conducted. From 5 to 14 days post-wounding, a great quantity of α7nAChR-positive myofibroblasts were observed in the contusion zones (Fig. 3). Morphometrically, the average ratios of α7nAChR-positive macrophages and myofibroblasts were shown in Fig. 4. The average ratios of α7nAChR-positive macrophages and myofibroblasts reached their climax at 3 and 7 days after injury, respectively.

Western blotting and real-time fluorescent quantitative PCR

The blots against α7nAChR and GAPDH antibody were shown in Fig. 5a. The average ratio of α7nAChR protein expression peaked at 7 days after contusion, which was >2.13. Besides, the ratios were <2.13 at the other posttraumatic intervals. The α7nAChR protein expression was increased from 12 h and decreased from 10 days after injury. Significant differences in the relative expression levels of α7nAChR protein were noted from 12 h to 14 days post-wounding, as compared with that of control. There were significant differences in the relative intensity of α7nAChR to GAPDH between 12 h, 1 day, 7 days, 10 days injury groups and their preceding groups as shown in Fig. 5b.

Relative quantity of α7nAChR mRNA expression in rat skeletal muscle was assayed by real-time PCR throughout the 14 days after contusion. Similar to Western blotting results, the relative quantity of α7nAChR mRNA expression reached peak levels and exceeded 2.65 at 7 days after injury, whereas it was <2.65 at the other posttraumatic intervals. Significant differences in the relative quantity of α7nAChR mRNA expression were observed from 6 h to 14 days post-wounding, as compared with control. There were significant differences in the relative quantity of α7nAChR mRNA expression between 6 h, 12 h, 1 day, 3 days, 5 days, 7 days, 10 days, 14 days injury groups and their preceding groups as shown in Fig. 6.

Table 2 Average ratio of α7nAChR-positive infiltrating cells in different periods (n=5)

Group	n	Positive cells ratio (%)
3 h	5	9.16±1.33
6 h	5	11.73±3.85
12 h	5	21.68±2.67*
1 day	5	43.25±2.96*
3 days	5	53.26±4.18*
5 days	5	62.35±4.32*
7 days	5	64.56±4.78
10 days	5	52.77±3.62*
14 days	5	37.13±3.39*

*p<0.05 (vs. preceding posttraumatic interval)

Discussion

The cholinergic system consists of ACh, mAChRs and nAChRs, ChAT, and AChE. In the past, most available information on cholinergic system was derived from researches on

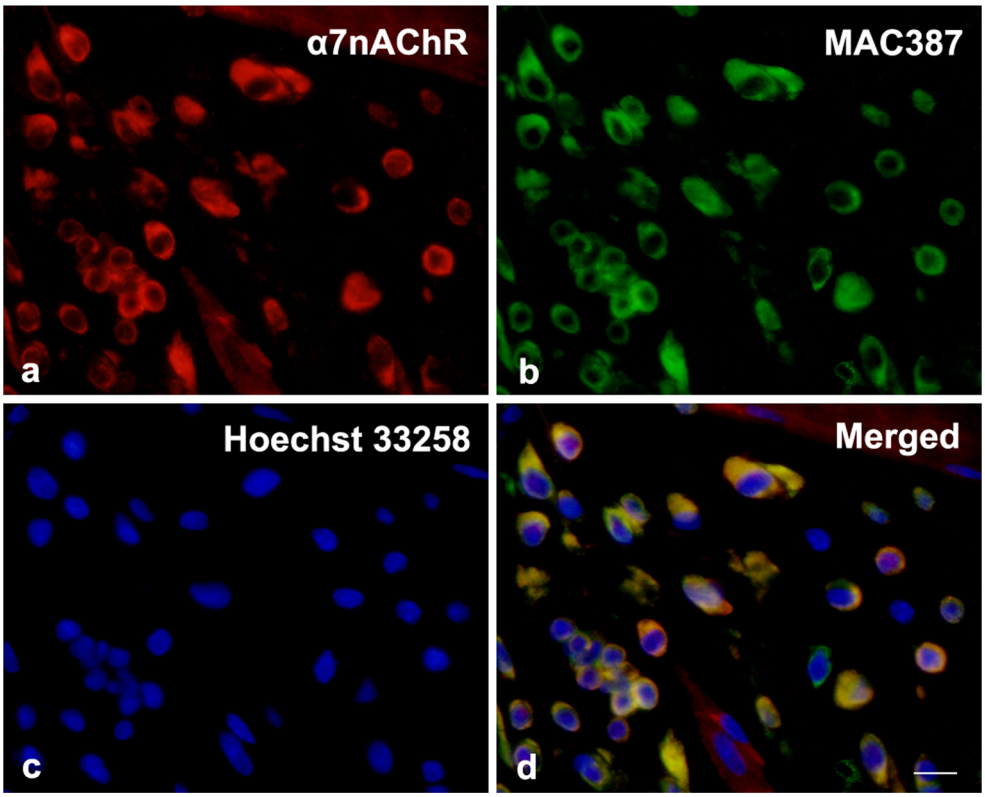

Fig. 2 Double immunofluorescence analysis was performed to determine α7nAChR-expressing macrophages at 3 days post-injury. The samples were immunostained with anti-α7nAChR (**a**, *red*) and anti-macrophage marker (MAC387) (**b**, *green*). Nuclei were counterstained with Hoechst33258 (**c**, *blue*). Signals in panels **a**, **b**, and **c** were digitally merged in panel **d**. Representative results from at least three independent experiments are shown here (*Scale bar*=10 μm)

the nervous systems of mammalian species [12]. Nonetheless, recent evidences have showed that cholinergic system exists in numerous nonneuronal cells and organs including skeletal muscle. It is proposed that almost all the life-forms on the earth appear to have the ability to synthesize ACh [22]. In the cholinergic system, α7nAChR mainly mediate the biological

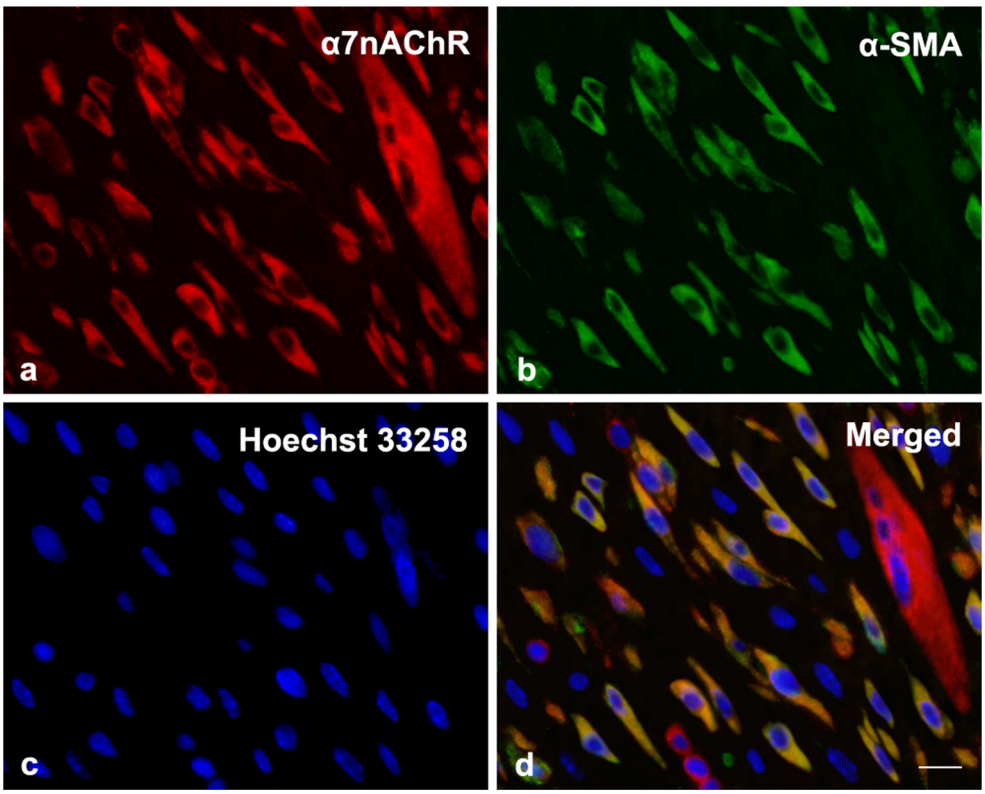

Fig. 3 Double immunofluorescence analysis was performed to determine α7nAChR-expressing myofibroblasts at 7 days post-injury. The samples were immunostained with anti-α7nAChR (**a**, *red*) and anti-myofibroblast marker (α-SMA) (**b**, *green*). Nuclei were counterstained with Hoechst33258 (**c**, *blue*). Signals in panels **a**, **b**, and **c** were digitally merged in panel **d**. Representative results from at least three independent experiments are shown here (*Scale bar*=10 μm)

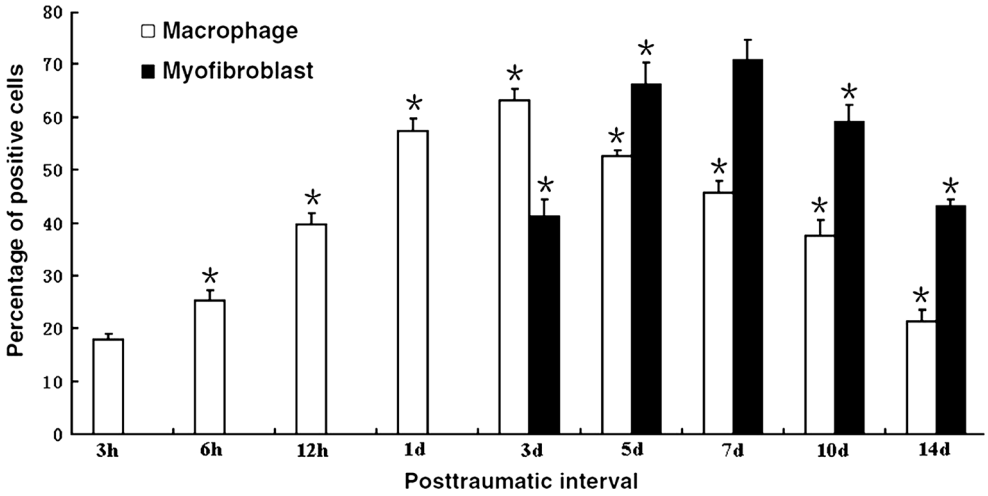

Fig. 4 Average ratios of α7nAChR-positive macrophages and myofibroblasts in relation to wound age. *$p<0.05$ (vs preceding posttraumatic group)

roles of ACh. Furthermore, choline as a precursor and the main degradation product of ACh is more stable and widely available and has a selective affinity to α7nAChR [12]. Actually, it is well established that inflammatory cells present a complete cholinergic system [22, 23]. Activation of α7nAChR on macrophages leads to efficient suppression of pro-inflammatory cytokine production, indicating promise in the treatment of inflammatory disorders [18, 24, 25]. Besides, α7nAChR can be expressed by fibroblasts and myofibroblasts, which are closely involved in collagen expression and myofibroblast differentiation [26, 27]. Skeletal muscle wound healing is composed of degeneration, inflammation, regeneration, and fibrosis phases [10]. Thus, it is considered that α7nAChR may be involved in inflammatory and fibrotic phases during skeletal muscle wound healing. The infiltrating cells such as leukocytes and fibroblasts should be morphometrically analyzed. According to the previous study, α7nAChR was mainly expressed by macrophages and myofibroblasts and was involved in the inflammatory response and fibrotic repair in skin wound healing [19]. Consistent with previous findings, the present study showed that MAC387-positive macrophages and α-SMA-positive myofibroblasts predominantly expressed α7nAChR in skeletal muscle contusion zones. To our knowledge, this is the first report to characterize localization of α7nAChR in macrophages and myofibroblasts during skeletal muscle wound healing.

In forensic practices, most researches regarding wound age determination were conducted by histopathology and immunohistochemistry [4, 5, 28–33]. In addition to judging wound age, it is beneficial to reveal the potentially biological mechanism of detected indexes by immunohistochemistry and

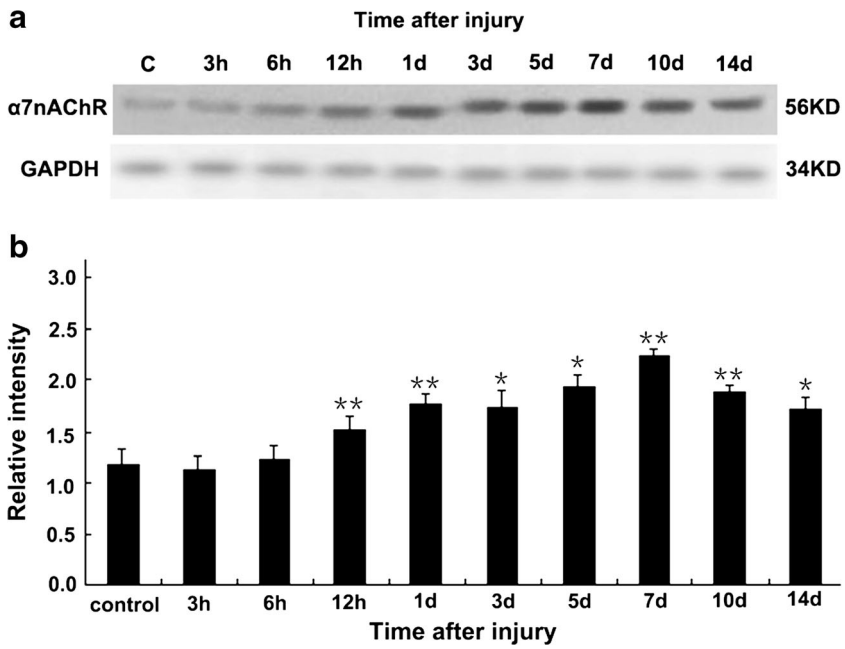

Fig. 5 **a** Analysis of α7nAChR and GAPDH protein from rat skeletal muscle specimens by Western blotting. Lane *C* represents the result of the control skeletal muscle sample. Representative results from five individual animals are shown. **b** Relative intensity of α7nAChR to GAPDH. All values are expressed as the means±SD ($n=5$). *$p<0.05$ (vs control group); **$p<0.05$ (vs control group or preceding posttraumatic group)

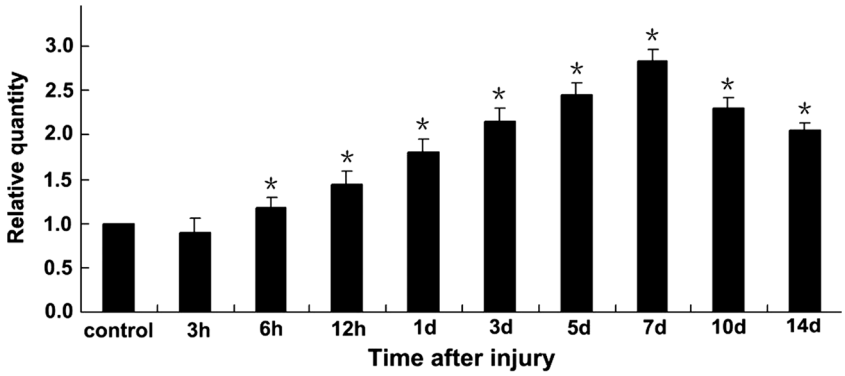

Fig. 6 Relative quantity of α7nAChR mRNA expression. All values are expressed as the means±SD (n=5). *p<0.05 (vs control group or preceding posttraumatic group)

morphometric analysis. However, some investigator considered that immunohistochemical results were not accurate and stable in quantitative analysis, and the results may be influenced by operator skills [2, 8, 9, 34, 35]. Recently, techniques of Western blotting and real-time PCR have been applied to wound age determination, implying that the more exact expression tendency for markers of wound age might be observed by Western blotting and real-time PCR [8, 9, 36]. Thus, the expression of α7nAChR was also examined by Western blotting and real-time PCR in the present study. Our data showed that the levels of α7nAChR increased in a time-dependent manner after contusion and peaked at 7 days post-wounding. From the viewpoint of forensic pathological applications, the α7nAChR-positive ratios of >50 % suggests a wound age of 3 to 10 days, and the positive ratios of >60 % possibly indicate a wound age of 5 to 7 days, as detected by immunohistochemical analysis. Moreover, an increasing expression of α7nAChR is sequentially detected in macrophages and myofibroblasts after injury. The ratio of α7nAChR-positive macrophages over 60 % possibly suggests a wound age of 3 days, and the ratio of α7nAChR-positive myofibroblasts over 65 % possibly indicates a wound age of 5 to 7 days. Furthermore, in Western blotting results, all samples in 7 days post-injury groups showed ratios of >2.13. Besides, no other posttraumatic intervals showed ratios of >2.13. Similarly, the tendency of α7nAChR mRNA expression by real-time PCR was almost identical with that of α7nAChR protein expression by Western blotting. The relative quantity of α7nAChR mRNA expression peaked at 7 days after injury, which was >2.65. When wound age was <12 h, there was significant difference in real-time PCR result between 3 and 6 h post-injury. Therefore, the present study indicates that α7nAChR is a useful marker in estimating skeletal muscle wound age.

In recent years, some markers of estimating wound age have been shown to display regular expressions following the injury [37–41]. Nevertheless, the positive reaction of markers must be based on quantitative data which are always debatable in court. Hence, it is necessary to examine the various parameters by combining different methods, so that the comprehensive results can minimize the error margin in time calculation [37]. With the development of PCR technique, it is proposed that a system for the determination of wound vitality should be established at the gene as well as protein level [38, 39]. According to previous researches [34, 36, 42], various proteins were synthesized after the induction of mRNA, and it was more appropriate to detect mRNA in early wound age estimation. Moreover, detection of protein and mRNA by Western blotting and RT-PCR was more suitable for judging wound age, which was usually more stable and sensitive than immunohistochemical assays [9]. Consistent with previous findings, our study suggests that biological markers simultaneously detected by the combination of real-time PCR, Western blotting, and morphological analysis may provide more accurate and objective parameters for wound age determination. As a result, the error margin of time estimation will be narrowed further.

In conclusion, we demonstrated an upregulated expression of α7nAChR during skeletal muscle wound healing in rats. After trauma to skeletal muscle, α7nAChR was temporally detected in macrophages and myofibroblasts, which might be involved in the inflammatory reaction and fibrotic repair after injury. Besides, the mRNA and protein levels of α7nAChR, detected by real-time PCR, Western blotting, and morphological analysis, would provide more solid information for wound age estimation. Finally, the present results were obtained from well-controlled animal experiments, providing the experimental evidence that α7nAChR is a useful marker in estimating skeletal muscle wound age. For forensic practical application, it is essential to collect human skeletal muscle samples with a variety of wound ages and further examine the suitability of α7nAChR in autopsy cases by real-time PCR, Western blotting, and morphological analysis.

Acknowledgment This study was financially supported in part by grants from research funds for Zhejiang Provincial Natural Science Foundation of China (Q13H150005) and National Natural Science Foundation of China (81301640).

References

1. Ishida Y, Kimura A, Nosaka M, Kuninaka Y, Takayasu T, Eisenmenger W, Kondo T (2012) Immunohistochemical analysis on cyclooxygenase-2 for wound age determination. Int J Legal Med 126:435–440
2. Takamiya M, Saigusa K, Kumagai R, Nakayashiki N, Aoki Y (2005) Studies on mRNA expression of tissue-type plasminogen activator in bruises for wound age estimation. Int J Leg Med 119:16–21
3. Sato Y, Ohshima T (2000) The expression of mRNA of proinflammatory cytokines during skin wound healing in mice: a preliminary study for forensic wound age estimation (II). Int J Leg Med 113:140–145
4. Kondo T, Ohshima T, Mori R, Guan DW, Ohshima K, Eisenmenger W (2002) Immunohistochemical detection of chemokines in human skin wounds and its application to wound age determination. Int J Legal Med 116:87–91
5. Hayashi T, Ishida Y, Kimura A, Takayasu T, Eisenmenger W, Kondo T (2004) Forensic application of VEGF expression to skin wound age determination. Int J Legal Med 118:320–325
6. Kagawa S, Matsuo A, Yagi Y, Ikematsu K, Tsuda R, Nakasono I (2009) The time-course analysis of gene expression during wound healing in mouse skin. Leg Med 11:70–75
7. Zhao R, Guan DW, Zhang W, Du Y, Xiong CY, Zhu BL, Zhang JJ (2009) Increased expressions and activations of apoptosis-related factors in cell signaling during incised skin wound healing in mice: a preliminary study for forensic wound age estimation. Leg Med 11: S155–S160
8. Sun JH, Wang YY, Zhang L, Gao CR, Zhang LZ, Guo Z (2010) Time-dependent expression of skeletal muscle troponin I mRNA in the contused skeletal muscle of rats: a possible marker for wound age estimation. Int J Legal Med 124:27–33
9. Yu TS, Cheng ZH, Li LQ, Zhao R, Fan YY, Du Y, Ma WX, Guan DW (2010) The cannabinoid receptor type 2 is time-dependently expressed during skeletal muscle wound healing in rats. Int J Legal Med 124:397–404
10. Prisk V, Huard J (2003) Muscle injuries and repair: the role of prostaglandins and inflammation. Histol Histopathol 18:1243–1256
11. Charge SB, Rudnicki MA (2004) Cellular and molecular regulation of muscle regeneration. Physiol Rev 84:209–238
12. Kurzen H, Wessler I, Kirkpatrick CJ, Kawashima K, Grando SA (2007) The non-neuronal cholinergic system of human skin. Horm Metab Res 39:125–135
13. Karlin A (2002) Emerging structure of the nicotinic acetylcholine receptors. Nat Rev Neurosci 3:102–114
14. Xiu J, Nordberg A, Zhang JT, Guan ZZ (2005) Expression of nicotinic receptors on primary cultures of rat astrocytes and upregulation of the alpha7, alpha4 and beta2 subunits in response to nanomolar concentrations of the beta-amyloid peptide (1-42). Neurochem Int 47: 281–290
15. Kummer W, Lips KS, Pfeil U (2008) The epithelial cholinergic system of the airways. Histochem Cell Biol 130:219–234
16. Liu RH, Mizuta M, Matsukura S (2004) The expression and functional role of nicotinic acetylcholine receptors in rat adipocytes. J Pharmacol Exp Ther 310:52–58
17. Metz CN, Tracey KJ (2005) It takes nerve to dampen inflammation. Nat Immunol 6:756–757
18. Su X, Lee JW, Matthay ZA, Mednick G, Uchida T, Fang X, Gupta N, Matthay MA (2007) Activation of the alpha7 nAChR reduces acid-induced acute lung injury in mice and rats. Am J Respir Cell Mol 37: 186–192
19. Fan YY, Yu TS, Wang T, Liu WW, Zhao R, Zhang ST, Ma WX, Zheng JL, Guan DW (2011) Nicotinic acetylcholine receptor α7 subunit is time-dependently expressed in distinct cell types during skin wound healing in mice. Histochem Cell Biol 135:375–387
20. Zhang ST, Zhao R, Ma WX, Fan YY, Guan WZ, Wang J, Ren P, Zhong K, Yu TS, Pi JB, Guan DW (2013) Nrf1 is time-dependently expressed and distributed in the distinct cell types after trauma to skeletal muscles in rats. Histol Histopathol 28:725–735
21. Fan YY, Ye GH, Lin KZ, Yu LS, Wu SZ, Dong MW, Han JG, Feng XP, Li XB (2013) Time-dependent expression and distribution of Egr-1 during skeletal muscle wound healing in rats. J Mol Histol 44:75–81
22. Kawashima K, Fujii T (2008) Basic and clinical aspects of non-neuronal acetylcholine: overview of non-neuronal cholinergic systems and their biological significance. J Pharmacol Sci 106:167–173
23. Kawashima K, Fujii T (2003) The lymphocytic cholinergic system and its contribution to the regulation of immune activity. Life Sci 74:675–696
24. Tracey KJ (2002) The inflammatory reflex. Nature 420:853–859
25. Wang H, Yu M, Ochani M, Amella CA, Tanovic M, Susarla S, Li JH, Wang H, Yang H, Ulloa L, Al-Abed Y, Czura CJ, Tracey KJ (2003) Nicotinic acetylcholine receptor alpha7 subunit is an essential regulator of inflammation. Nature 421:384–388
26. Sekhon HS, Keller JA, Proskocil BJ, Martin EL, Spindel ER (2002) Maternal nicotine exposure upregulates collagen gene expression in fetal monkey lung. Association with alpha7 nicotinic acetylcholine receptors. Am J Respir Cell Mol Biol 26:31–41
27. Rehan VK, Wang Y, Sugano S, Romero S, Chen X, Santos J, Khazanchi A, Torday JS (2005) Mechanism of nicotine-induced pulmonary fibroblast transdifferentiation. Am J Physiol Lung Cell Mol Physiol 289:L667–L676
28. Betz P (1994) Histological and enzyme histochemical parameters for the age estimation of human skin wounds. Int J Legal Med 107:60–68
29. Kondo T, Tanaka J, Ishida Y, Mori R, Takayasu T, Ohshima T (2002) Ubiquitin expression in skin wounds and its application to forensic wound age determination. Int J Legal Med 116:267–272
30. Ishida Y, Kimura A, Takayasu T, Eisenmenger W, Kondo T (2008) Expression of oxygen-regulated protein 150 (ORP150) in skin wound healing and its application for wound age determination. Int J Legal Med 122:409–414
31. Ishida Y, Kimura A, Takayasu T, Eisenmenger W, Kondo T (2009) Detection of fibrocytes in human skin wounds and its application for wound age determination. Int J Legal Med 123:299–304
32. Kondo T, Ohshima T, Eisenmenger W (1999) Immunohistochemical and morphometrical study on the temporal expression of interleukin-1α (IL-1α) in human skin wounds for forensic wound age determination. Int J Legal Med 112:249–252
33. Betz P (1995) Immunohistochemical parameters for the age estimation of human skin wounds. A review. Am J Forensic Med Pathol 16: 203–209
34. Bai R, Wan L, Shi M (2008) The time-dependent expressions of IL-1beta, COX-2, MCP-1 mRNA in skin wounds of rabbits. Forensic Sci Int 175:193–197
35. Zheng JL, Yu TS, Li XN, Fan YY, Ma WX, Du Y, Zhao R, Guan DW (2012) Cannabinoid receptor type 2 is time-dependently expressed during skin wound healing in mice. Int J Legal Med 126:807–814
36. Ma WX, Yu TS, Fan YY, Zhang ST, Ren P, Wang SB, Zhao R, Pi JB, Guan DW (2011) Time-dependent expression and distribution of monoacylglycerol lipase during the skin-incised wound healing in mice. Int J Legal Med 125:549–558
37. Cecchi R (2010) Estimating wound age: looking into the future. Int J Legal Med 124:523–536
38. Kondo T (2007) Timing of skin wounds. Leg Med (Tokyo) 9:109–114
39. Ohshima T (2000) Forensic wound examination. Forensic Sci Int 113:153–164
40. Hernández-Cueto C, Girela E, Sweet DJ (2000) Advances in the diagnosis of wound vitality: a review. Am J Forensic Med Pathol 21:21–31
41. Oehmichen M (2004) Vitality and time course of wounds. Forensic Sci Int 144:221–231
42. Ohshima T, Sato Y (1998) Time-dependent expression of interleukin-10 (IL-10) mRNA during the early phase of skin wound healing as a possible indicator of wound vitality. Int J Leg Med 111:251–255